Determination of effective mass in InN by high-field oscillatory magnetoabsorption spectroscopy

Marius Millot,[1,2,3,*] Nicolas Ubrig,[1,2] Jean-Marie Poumirol,[1,2] Iulian Gherasoiu,[4] Wladek Walukiewicz,[5] Sylvie George,[1,2] Oliver Portugall,[1,2] Jean Léotin,[1,2] Michel Goiran,[1,2] and Jean-Marc Broto[1,2]

[1]*Université de Toulouse; UPS, INSA, 143 Avenue de Rangueil, F-31400 Toulouse, France*

[2]*Laboratoire National des Champs Magnétiques Intenses (LNCMI) – CNRS UPR 3228, 143 Avenue de Rangueil, F-31400 Toulouse, France*

[3]*Department of Earth and Planetary Science, University of California-Berkeley, Berkeley, California 94720, USA*

[4]*RoseStreet Labs Energy, 3701 E. University Drive, Phoenix, Arizona 85034, USA*

[5]*Materials Sciences Division, Lawrence Berkeley National Laboratory, Berkeley, California 94720, USA*

(Received 17 March 2010; revised manuscript received 23 November 2010; published 18 March 2011)

We report on oscillatory magnetoabsorption experiments on several indium nitride (InN) epilayers under a pulsed magnetic field up to 56 T. This optical technique is uniquely suited to probe the bulk electronic structure in the vicinity of the fundamental band edge by Landau level spectroscopy. We discuss these results in light of two recent studies on the InN band structure by high-field magnetotransport [Goiran *et al.*, Appl. Phys. Lett. **96**, 052117 (2010)] and magneto-photoluminescence [Pettinari *et al.*, Phys. Rev. B **79**, 165207 (2009)]. In particular, we evidence a strong nonparabolicity of the conduction band and demonstrate that the electron effective mass $m^*_{e\perp 0} = 0.055m_0$ measured by Shubnikov–de Haas oscillations is confirmed by the magneto-optical experiments.

DOI: 10.1103/PhysRevB.83.125204 PACS number(s): 71.18.+y, 71.20.Nr, 73.61.Ey, 78.20.Ls

I. INTRODUCTION

InN and its alloys with other III-nitride materials (GaInN, AlInN, AlGaInN) have received very strong interest since the revision of the admitted value of the indium nitride band-gap energy from 1.9 eV to ∼0.7 eV. The low gap of InN greatly expanded the range of the direct gaps of the group III-N alloys and offered an outstanding potential for solar energy conversion and optoelectronic applications.[1,2] As a narrow gap semiconductor InN is expected to have a low electron effective mass m^*_e and thus a high mobility μ_e. This is very promising for the design of fast electronic and optoelectronic devices in the future.

Despite intense worldwide effort, many InN fundamental properties, such as the detailed electronic structure near the conduction band edge, still remain poorly understood. Experimental investigations have been hampered for years by the difficulty to grow high-quality crystals of InN and the existence of an intrinsic low mobility surface and/or interface electron accumulation layer[3,4] that affects the electrical and optical properties of this material and thereby any measurement relying on surface properties. In addition, only recent sophisticated *ab initio* band structure simulations have been able to provide a complete picture in agreement with the available experimental values for the energy gap and band parameters.

The reported values of m^*_e span between $0.044m_0$ and $0.093m_0$.[5–9] A more recent *ab initio* comprehensive study determined the band structure parameters including electron effective mass of $m^*_e = 0.068m_0$.[10] Most of these measurements have been performed by surface sensitive methods, such as infrared reflectance[6,7] or ellipsometry,[8] that require complex analysis procedures. Recent magneto-optical measurements of interband Landau level (LL) magneto-photoluminescence (MPL) under strong magnetic field up to 30 T lead Pettinari and co-workers to conclude that the electron effective mass in degenerate InN is higher than $0.093m_0$[9]. These authors attribute the high effective mass to a strong modification of the band structure close to the Γ point due to the sources of the unintentional *n* doping. In addition, several authors of the present article have performed magnetotransport LL spectroscopy measurements under a pulsed magnetic field up to 56 T.[11] The thermal damping of the Shubnikov–de Haas (SdH) oscillations provides a bulk electron cyclotron effective mass $0.062 \pm 0.002m_0$ at the Fermi level. This corresponds to a bare band edge electron mass of $0.055 \pm 0.002m_0$ when corrected for the finite carrier concentration and polaron contributions.

In this article, we present oscillatory magnetoabsorption (OMA) data on three indium nitride epilayers characterized under a pulsed magnetic field up to 56 T. We discuss these results in light of the most recent studies by SdH[11] and magneto-PL (MPL)[9] and propose an unifying interpretation for these experiments. In particular, we evidence a strong nonparabolicity of the conduction band and demonstrate that the electron effective mass measured by Shubnikov–de Haas oscillations is confirmed by the magneto-optical experiments.

II. METHODS

Indium nitride crystals were grown by plasma-assisted molecular beam epitaxy (MBE) on c-plane sapphire substrates with a GaN buffer layer using an adaptive deposition technique known as metal modulation epitaxy to control the unintentional doping due to nitrogen vacancies. More details about the sample growth can be found elsewhere.[11,12] Samples were characterized using photoluminescence and Hall measurements at room and liquid-nitrogen temperature. The carrier concentration are in the 10^{18} cm^{-3} range (see Table I). A specific setup with custom-made optical fiber probes was used to measure the optical absorption under pulsed magnetic field, in the Faraday configuration and with $B \parallel c$ (see Fig. 1) at 77 K.[13] A halogen light source and a fast InGaAs detector array coupled to a 0.3 m focal length spectrometer allowed to collect a full spectrum of the transmitted light through the sample every 4 ms with a 3.5 ms accumulation time during the exponential decay of the magnetic field

TABLE I. Sample characteristics and results summary: Hall concentration and mobility at 300 K; photoluminescence peak energy at 300 K; electron cyclotron effective mass $m^*_{e\perp}$ obtained by Shubnikov–de Haas (SdH) (sample A corresponds to S1 and D to S2 in Ref. 11); energy gap E_g and reduced effective mass $\mu_\perp$ extracted from OMA assuming a linear conduction band (CB), i.e., a linear LL analysis; band parameters derived from the nonlinear LL analysis assuming a linear valence band with curvature $-m^*_{h\perp}$ lying E_g below the bottom of a nonparabolic CB characterized by Ep or equivalently by the electron effective mass at the bottom of the band $m^*_{e\perp 0}/m_0 = 1/(1 + Ep/E_g)$ in the framework of Eq. (4).

	Hall effect		Photoluminescence	Shubnikov–de Haas	OMA Parabolic CB		OMA Nonparabolic CB			
Sample	n_H 10^{18} cm^{-3}	Mobility cm^2/V · s	Peak energy eV	$m^*_{e\perp}$ m_0	E_g eV	$\mu^*_{\perp 0}$ m_0	E_g eV	Ep eV	$m^*_{h\perp}$ m_0	$m^*_{e\perp 0}$ m_0
A	1.94	1900	0.645	0.055	–	–	–	–	–	–
B	2.00	1800	0.655	–	0.71	0.091	0.658	11.3	2.8	0.055
C	3.20	1400	0.654	–	0.70	0.090	0.655	11.3	2.44	0.055
D	3.57	1570	0.654	0.055	0.70	0.089	0.655	11.3	2.3	0.055

pulse (∼250 ms). Unfortunately, as our detector cutoff was 1600 nm we were not able to measure simultaneously the magneto-photoluminescence signal centered around 1900 nm at 300 K.

III. RESULTS

The inset of Fig. 2 shows the band edge absorption spectrum of sample D recorded at zero field using a conventional Fourier Transform Infrared (FTIR) spectrometer. This spectrum is in good agreement with the previous report of absorption measurements[14,15] on InN crystals with concentration ∼10^{18}–10^{19} cm^{-3} and a linear extrapolation of α^2 gives an estimation for the band gap energy $Eg = 0.69$ eV.

Under strong magnetic field, above 20 T, several bands of absorption with magnetic-field-dependent energy appear progressively in our spectrally accessible window (0.77 eV–1.1 eV). Note the strong perturbation of the absorption coefficient in the contour plot of Fig. 1 showing the transmitted light intensity normalized with respect to the intensity of light at zero field as a function of the applied magnetic field. Typical spectra of transmitted light through the InN epilayer B at selected values of the applied magnetic field up to 56 T are also displayed in Fig. 2. The oscillatory magnetoabsorption (OMA) is a clear signature of the Landau quantization, and the observed intensity bands are related to interband transitions between LLs of holes in the valence band and electrons in the conduction band (see inset of Fig. 1). A similar behavior has already been observed in a wide variety of

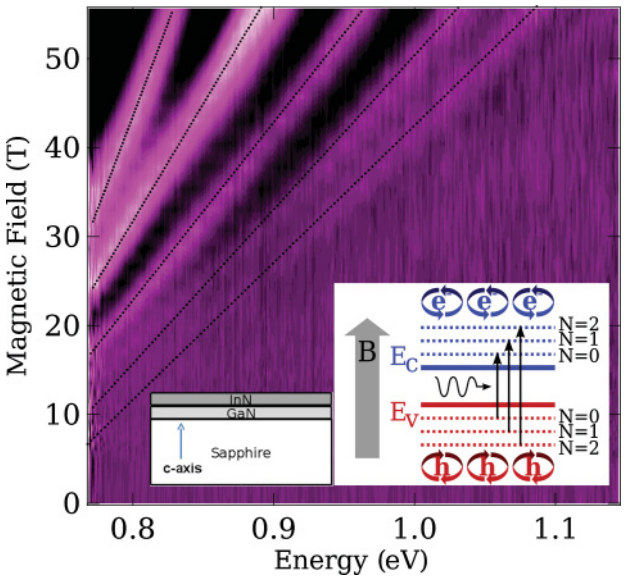

FIG. 1. (Color online) Contour plot of the transmitted light intensity divided by the zero-field intensity as a function of the applied magnetic field up to 56 T. Black corresponds to a high transmission. Left inset: Investigated samples side view with a 1 μm InN epilayer on a thin GaN buffer layer. Right inset: Schematic view of the present oscillatory magnetoabsorption experiments: under a strong magnetic field a photon can be preferentially absorbed if its energy matches the energy gap between an orbiting hole and an orbiting electron belonging to Landau levels with the same quantum number N.

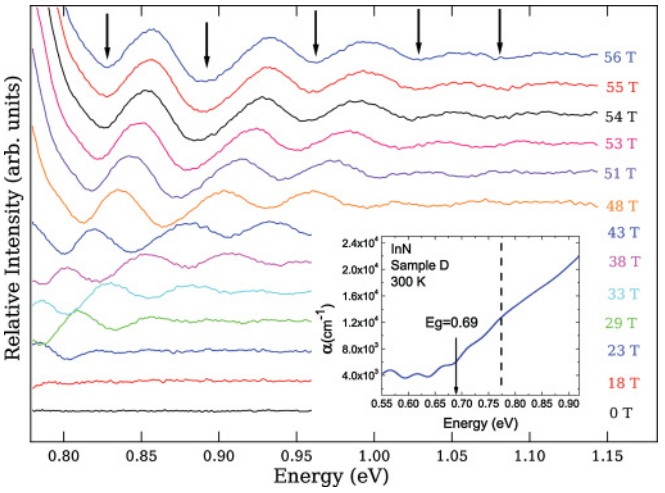

FIG. 2. (Color online) Normalized spectra of transmitted light through the InN crystal B at selected values of the applied magnetic field up to 56 T. Arrows indicate the OMA bands. Inset: Room temperature band-edge absorption spectrum of sample D recorded at zero field. The extrapolated value of the band gap (arrow) and the cut-off energy (dotted line) of the spectrometer used to record the OMA spectra are indicated.

cubic semiconductors, such as InAs, Ge and InSb,[17,18] GaAs,[19] or InP,[20] and layered hexagonal compounds like GaSe[21] and InSe.[13] The conservation law for the angular momentum yields strong selection rules for such interband LL transitions, which depend on the adopted model.[16] To extract information from the experimental data we draw a fan chart: OMA band center energy versus applied magnetic field. A fan chart gathering the data on our three samples is shown in Fig. 3(a).

IV. DISCUSSION

In a simplified approach we assume two perfectly parabolic noninteracting bands, with m_h^* ($m_h^* > 0$) and m_e^* effective masses separated by an energy gap E_g. The transition energies are obtained assuming direct, symmetry-allowed interband transitions satisfying the selection rule $\Delta N = 0$.[16] The transition energies are given by

$$E_{\mathrm{OMA}}(N,B) = E_g + \left(N + \tfrac{1}{2}\right)\hbar\omega_c \qquad (1)$$

with the reduced cyclotron angular frequency $\omega_c = \frac{eB}{m_0\mu^*}$ and the reduced effective mass

$$\frac{1}{\mu} = \frac{1}{m_h^*} + \frac{1}{m_e^*}. \qquad (2)$$

Is this simple framework, the LLs are linear. As a matter of fact, the fan chart in Fig. 3(a) shows such a roughly linear behavior. Going one step further and using

$$\tilde{B} = \left(N + \frac{1}{2}\right)\frac{\hbar eB}{m_0} \qquad (3)$$

to renormalize the magnetic field, the energies of the different transitions now are $E_{\mathrm{OMA}}(\tilde{B}) = E_g + \frac{1}{\mu_\perp}\tilde{B}$ and all the data points of the fan chart collapse on a single curve in the $E(\tilde{B})$ plane as shown in Fig. 3(b).[23] A linear regression provides a qualitative agreement, even if the data appear slightly scattered around the linear best fit (dotted black line). The values of $E_g = 0.70 \pm 0.01$ eV and $\mu_\perp = 0.090 \pm 0.001 m_0$ obtained from this analysis are listed in Table I. The reduced effective mass of $\mu_\perp \simeq 0.09 m_0$ is in a good agreement with the previous MPL study[9] carried out on samples in the same range of electron concentrations. This would establish a lower limit for the electron effective mass for degenerate InN $m_{e\perp}^* > 0.09 m_0$ in contrast with straightforward SdH measurements on similar samples[11] (giving a cyclotron effective mass at the bottom of the band $m_{e\perp 0}^* = 0.055 m_0$) and *ab initio* calculations (OEPx + G_0W_0 : $m_{e\perp}^* = 0.068 m_0$,[10] LDA + U : $m_{e\perp}^* = 0.05 m_0$[22]).

However, we demonstrate hereafter that, in fact, our magneto-optical experiments are in agreement with the electron effective mass measured by Shubnikov–de Haas oscillations.[11] We show that the discrepancy between the SdH results and the linear LL analysis of the OMA data actually unravels the strength of the nonparabolicity of the conduction band. Hence, we believe that the simple approach of parabolic bands is not suitable to describe this peculiar, narrow band, hexagonal wurtzite semiconductor and propose a unifying interpretation of both OMA and SdH data based on Kane's $\mathbf{k}\cdot\mathbf{p}$ nonparabolic dispersion relation introduced by Wu *et al.*[5]

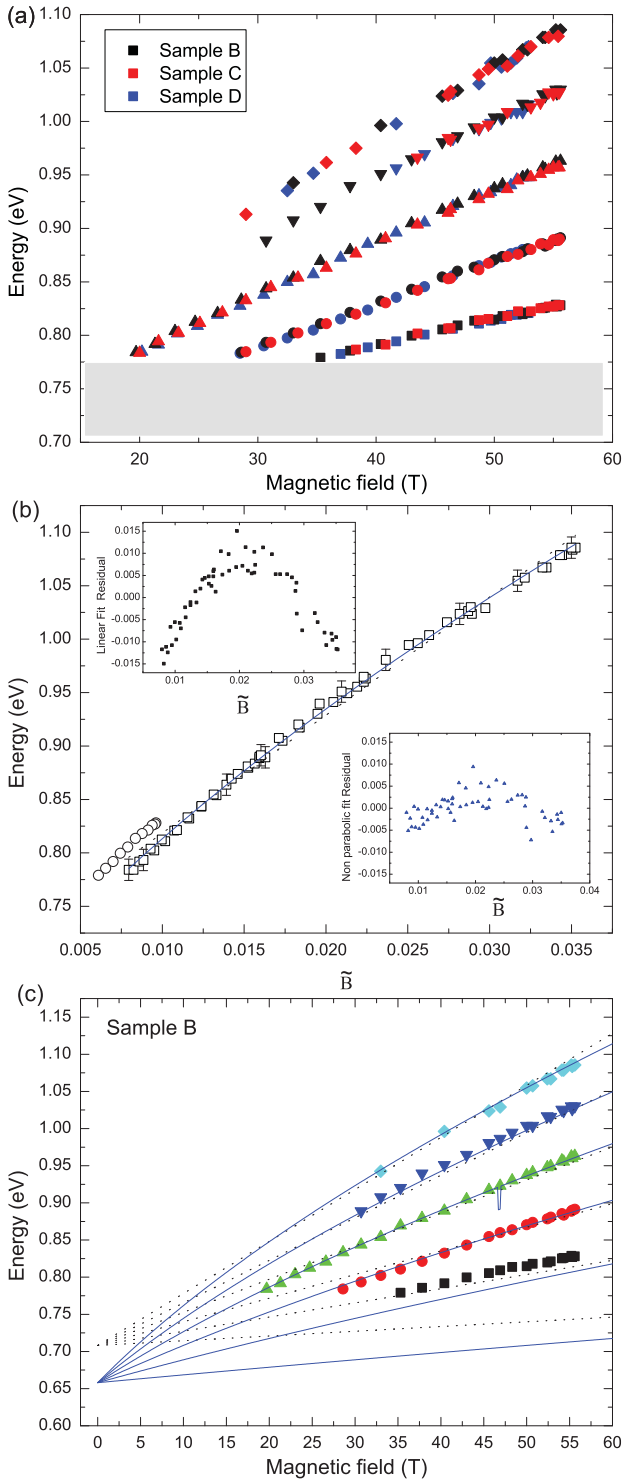

FIG. 3. (Color online) (a) OMA fan chart of the three InN samples, measured at 77 K. The nonaccessible energy range appears in light grey. (b) OMA band energies as a function of the renormalized magnetic field $\tilde{B} = (N + 1/2)\hbar eB/m_0$ for sample B. The circles have been disregarded for the fit procedure.[23] Linear best fit is shown as a black dotted line. Nonlinear best fit is based on Eq. (7) with the electron effective mass value at the bottom of the band $m_{e\perp 0}^* = 0.055 m_0$ (solid blue line). Left inset: Residual of the linear fit. Right inset: Residual of the nonlinear fit. (c) Measured OMA energies for sample B and calculated values using the results of the linear (black dotted line) and nonlinear (solid blue line) fits.

In fact, the linear LL analysis does not capture all the details of the experimental data and thus leads to an erroneous conclusion. Note the clear nonmonotonic magnetic field dependence of the residual values of the least-squares fit shown in the upper left inset of Fig. 3(b). As a consequence, the calculated OMA transitions corresponding to this fit drawn on Fig. 3(c) (dotted lines) are, in fact, only in rough agreement with the experimental data. The sublinear increase of the OMA band energies with respect to the magnetic field suggests that the conduction band nonparabolicity plays a key role here and must be taken into account.

Actually, infrared plasma frequency[5] and optical absorption experiments[14] have demonstrated that the conduction band (CB) is not parabolic, as expected for such a narrow gap compound allowing a noticeable mixing between the lowermost conduction band and the uppermost valence bands. Wu *et al.* have proposed a dispersion relation for the conduction band, in a simple, quasicubic, $2 \times 2\,\mathbf{k} \cdot \mathbf{p}$ framework neglecting the spin degeneracy[5]:

$$E_C(k) = \frac{E_g}{2} + \frac{\hbar^2 k^2}{2m_0} + \sqrt{\left(\frac{E_g}{2}\right)^2 + E_p \frac{\hbar^2 k^2}{2m_0}}. \qquad (4)$$

E_p describes the curvature of the band and includes the $\mathbf{k} \cdot \mathbf{p}$ mixing. The electron effective mass at the bottom of the band $m^*_{e0} = (1 + E_p/E_g)^{-1}$. Reported values range from 8.81 eV[10] to 10 eV[5] and 12 eV.[11] Using the quantization rule $\frac{\hbar^2 k^2}{2m_0} \rightarrow \frac{\hbar eB}{m_0}(N + \frac{1}{2})$ we obtain the LL energy as a function of the magnetic field:

$$E_C(N,B) = \frac{E_g}{2} + \left(N + \frac{1}{2}\right)\frac{\hbar eB}{m_0} + \sqrt{\left(\frac{E_g}{2}\right)^2 + E_p\left(N + \frac{1}{2}\right)\frac{\hbar eB}{m_0}}. \qquad (5)$$

In this nonparabolic approximation, the electron LLs are then unevenly spaced at high magnetic field and high energy above the bottom of the band. The effective mass energy dependence leads to a sublinear increase of the LL energy with respect to the magnetic field. Again, we can use Eq. (3) to obtain the major curve equation for the electron LLs as a function of $\tilde{B}$:

$$E_C(\tilde{B}) = \frac{E_g}{2} + \tilde{B} + \sqrt{\left(\frac{E_g}{2}\right)^2 + E_p \tilde{B}}. \qquad (6)$$

Using the nonparabolic dispersion for the CB and assuming single parabolic valence band,[25] the OMA bands are now given by

$$E_{\mathrm{OMA}}(\tilde{B}) = \frac{E_g}{2} + \left(1 + \frac{1}{m^*_h}\right)\tilde{B} + \sqrt{\left(\frac{E_g}{2}\right)^2 + E_p \tilde{B}}. \qquad (7)$$

Therefore, the higher the OMA band energy, the more important we expect the nonparabolicity effects. In fact, a sublinear increase is clearly evidenced in the fan chart plot in Fig. 3(a) and 3(b).

We have then also performed a nonlinear fit of the data using Eq. (7). A very good agreement is found assuming the electron effective mass value at the bottom of the band $m^*_{e\perp 0} = 0.055 m_0$ provided by the SdH study[11] on similar samples.[24] The best fit and the plot of residual values are displayed in Fig. 3(b) (respectively, dashed line and squares). The residual spread is slightly smaller and its distribution better approaches a random pattern when compared with the linear LL fit. The corresponding OMA energies are also plotted in Fig. 3(c): notice the improved very good agreement between the calculated and measured OMA energies. We obtain $E_g = 0.66$ eV and $m^*_{h\perp} \simeq 2.5 m_0$ (see Table I). We thereby demonstrate that our refined analysis based on the nonparabolic dispersion relation given in Eq. (4) accounts well for the observed OMA behavior and provides a set of reasonable parameters for the InN electronic structure at the vicinity of the fundamental band edge. Altogether, the results of the analysis based on Eqs. (4) and (7) provide a good description of the experimental OMA results in agreement with previous SdH and numerical studies of the band structure.

The large hole effective mass suggested by this analysis may reflect the peculiar valence band structure of this wurtzite hexagonal compound with three quasidegenerate valence bands. The crystal field Δ_{CR} and spin-orbit Δ_{SO} splitting parameters are not well established and the values quoted in the literature differ widely. Early calculations suggest $\Delta_{\mathrm{CR}} =$ 41 meV and $\Delta_{\mathrm{SO}} = 1$ meV,[26] near-edge optical absorptions provide $\Delta_{\mathrm{CR}} = 19$–$24$ meV using $\Delta_{\mathrm{SO}} = 5$ or 13 meV given by different simulations[27,28] when *ab initio* calculations[10] reproducing correctly the band-gap energy suggest $\Delta_{\mathrm{CR}} = 66$ meV neglecting the spin, i.e., $\Delta_{\mathrm{SO}} \approx 0$.

Note that a reliable prediction of the effective masses, i.e., of the bands curvatures around $k = 0$, is extremely difficult. Molina-Sanchez *et al.* recently obtained, with density-functional-theory-based numerical methods and tight binding parametrization,[29] $m^*_{h\perp A} = 2.8 m_0$, $m^*_{h\perp B} = 0.07 m_0$, and $m^*_{h\perp C} = 0.57 m_0$. The degenerate A and B valence bands belong to the Γ_{6v} representation and are mostly p type when the conduction band at Γ belongs to Γ_{1v} and is s type. These results match perfectly with our analysis suggesting that the OMA bands would originate from the A band. In contrast, according to Rinke *et al.*[10] the effective masses around Γ in the plane perpendicular to the c axis for the uppermost valence bands A and B are $m^*_{h\perp A} \approx m^*_{h\perp B} = 0.131 m_0$ and $m^*_{h\perp C} \approx 2 m_0$ for the C band, but there is no experimental evidence for these predictions. Besides, with splitting parameters ~10–30 meV comparable to the holes cyclotron energies, we can expect a mixing of the bands under high magnetic field which can result in a complex spectrum of holes LLs and an apparent effective mass as high as $2m_0$ for the holes. Actually, an exact derivation of the LLs in the case of GaN has recently been performed and has unraveled holes LL mixing.[30]

V. CONCLUSIONS

To summarize, we have presented oscillatory magnetoabsorption experiments up to 56 T on three MBE grown indium nitride epilayers. The magneto-fingerprints match well with the recent Shubnikov–de Haas determination of the electron effective mass and provide additional proof of the strong nonparabolicity of the conduction band. We hope that this study will stimulate both numerical calculations and

further experiments. In particular, uniaxial stress dependent, circularly polarized magneto-optical measurements would be extremely interesting to unravel the details of the band structure, a milestone toward *p*-doped InN devices.[31]

ACKNOWLEDGMENTS

The authors acknowledge D. Charrier and S. Nanot for stimulating discussions. Part of this work was supported by EuroMagNET II at LNCMI-T facility.

*millot.marius@gmail.com

[1] J. Wu, J. Appl. Phys. **106**, 011101 (2009), and reference therein.
[2] L. A. Reichertz, I. Gherasoiu, K. M. Yu, V. M. Kao, W. Walukiewicz, and J. W. Ager, Appl. Phys. Express **2**, 122202 (2009).
[3] H. Lu, W. J. Schaff, L. F. Eastman, and C. E. Stutz, Appl. Phys. Lett. **87**, 1736 (2003).
[4] L. Colakerol, T. D. Veal, H.-K. Jeong, L. Plucinski, A. DeMasi, T. Learmonth, P.-A. Glans, S. Wang, Y. Zhang, L. F. J. Piper, P. H. Jefferson, A. Fedorov, T.-C. Chen, T. D. Moustakas, C. F. McConville, and K. E. Smith, Phys. Rev. Lett. **97**, 237601 (2006).
[5] J. Wu, W. Walukiewicz, W. Shan, K. M. Yu, J. W. Ager, E. E. Haller, H. Lu, and W. J. Schaff, Phys. Rev. B **66**, 201403(R) (2002).
[6] S. P. Fu and Y. F. Chen, Appl. Phys. Lett. **85**, 1523 (2004).
[7] T. Inushima, M. Higashiwaki, and T. Matsui, Phys. Rev. B **68**, 235204 (2003).
[8] T. Hofmann, V. Darakchieva, B. Monemar, H. Lu, W. J. Schaff, and M. Schubert, J. Electron. Mater. **37**, 611 (2008).
[9] G. Pettinari, A. Polimeni, M. Capizzi, J. H. Blokland, P. C. M. Christianen, J. C. Maan, V. Lebedev, V. Cimalla, and O. Ambacher, Phys. Rev. B **79**, 165207 (2009).
[10] P. Rinke, M. Winkelnkemper, A. Qteish, D. Bimberg, J. Neugebauer, and M. Scheffler, Phys. Rev. B **77**, 075202 (2008), and references therein.
[11] M. Goiran, M. Millot, J. M. Poumirol, I. Gherasoiu, W. Walukiewicz, and J. Leotin, Appl. Phys. Lett. **96**, 052117 (2010).
[12] I. Gherasoiu, M. O'Steen, T. Bird, D. Gotthold, A. Chandolu, D. Y. Song, S. X. Xu, M. Holtz, S. A. Nikishin, and W. J. Schaff, J. Vac. Sci. Technol. A **26**, 399 (2008).
[13] M. Millot, J. M. Broto, S. George, J. Gonzalez, and A. Segura, Phys. Rev. B **81**, 205211 (2010).
[14] J. Ibanez, A. Segura, F. J. Manjon, L. Artus, T. Yamaguchi, and Y. Nanishi, Appl. Phys. Lett. **96**, 201903 (2010).
[15] S. X. Li, J. Wu, W. Walukiewicz, W. Shan, E. E. Haller, H. Lu, W. J. Schaff, Y. Saito, and Y. Nanishi, Phys. Status Solidi B **241**, 3107 (2004).
[16] N. Miura, *Physics of Semiconductors in High Magnetic Fields*, Vol. 15 of Semiconductor Science and Technology (Oxford University Press, New York, 2008).
[17] S. Zwerdling, B. Lax, L. M. Roth, and K. J. Button, Phys. Rev. **114**, 80 (1959).
[18] L. M. Roth, B. Lax, and S. Zwerdling, Phys. Rev. **114**, 90 (1959).
[19] Q. H. F. Vrehen, J. Phys. Chem. Solids **29**, 129 (1969).
[20] P. Rochon and E. Fortin, Phys. Rev. B **12**, 5803 (1975).
[21] K. Watanabe, K. Uchida, and N. Miura, Phys. Rev. B **68**, 155312 (2003).
[22] A. Terentjevs, A. Catellani, D. Prendergast, and G. Cicero, Phys. Rev. B **82**, 165307 (2010).
[23] The energy of the lowest measured OMA transition appears to be systematically higher that the expected one from the global fit of all the other data. We believe that this is an artefact: a consequence of the vicinity of the expected energy 0.7–0.8 eV with the brutal cutoff of our experimental setup.
[24] The crystals investigated in this study and the ones used in the SdH experiments pertain to the same series. Sample B is almost similar to A which was labeled S1 in Ref. 11 and sample D was labeled S2.
[25] As the hole effective mass is much larger than the electron effective mass, the hole cyclotron energies are much smaller than the electron ones. Hence the holes explore a narrower energy domain away from the valence band maximum and the VB nonparabolicity is expected to have a smaller impact on the OMA energies.
[26] S. H. Wei and A. Zunger, Appl. Phys. Lett. **69**, 2719 (1996).
[27] P. Carrier and S. H. Wei, J. Appl. Phys. **97**, 033707 (2005).
[28] R. Goldhahn, P. Schley, A. T. Winzer, M. Rakel, C. Cobet, N. Esser, H. Lu, and W. J. Schaff, J. Cryst. Growth **288**, 273 (2006).
[29] A. Molina-Sánchez, A. García-Cristóbal, A. Cantarero, A. Terentjevs, and G. Cicero, Phys. Rev. B **82**, 165324 (2010).
[30] M. Sobol and W. Bardyszewski, Phys. Rev. B **73**, 075208 (2006).
[31] N. Miller, J. W. Ager, H. M. Smith, M. A. Mayer, K. M. Yu, E. E. Haller, W. Walukiewicz, W. J. Schaff, C. Gallinat, G. Koblmuller, and J. S. Speck, J. Appl. Phys. **107**, 113712 (2010).